SCIENCE CHINA
Information Sciences

• RESEARCH PAPERS •

July 2011 Vol. 54 No. 7: 1534–1546
doi: 10.1007/s11432-011-4236-5

Range ambiguity resolving of HPRF radar based on hybrid filter

WANG Na[1,2*], WANG GuoHong[1], ZENG JiaYou[1] & HE You[1]

[1]*Naval Aeronautical and Astronautical University, Yantai* 264001*, China;*
[2]*Unit* 92941, 93 *Element, Huludao* 125001*, China*

Received January 15, 2010; accepted February 5, 2010; published online April 13, 2011

Abstract In this paper, a novel method of range ambiguity resolving based on hybrid filter is proposed for high-pulse repetition frequency (HPRF) radars. By considering the discrete-valued pulse interval number (PIN) which is described as the radial range of the target divided by the maximum unambiguous range for a certain HPRF and its incremental variable as target states, the problem of range ambiguity resolving is converted to the hybrid state estimation problem. In the initial time steps, since the range measurement is ambiguous, the hybrid state initialization is achieved by utilizing multiple HPRFs based on Euclidean distance. Then, to avoid the choice of the thresholds, the hybrid model based on six-dimension state vector is made equivalent to several hybrid models based on five-dimension state vector according to the values that PIN incremental variable may take. The hybrid estimation is achieved by comparing 2-norm of the innovations obtained from several hybrid filters. Simulation results demonstrate that the proposed method can converge more rapidly than the existing multiple hypothesis method when only one HPRF has target measurement and overcome the mistake that multiple hypothesis method makes when PIN varies.

Keywords HPRF, range ambiguity, pulse interval number, Euclidean distance, hybrid filter, innovation

Citation Wang N, Wang G H, Zeng J Y, et al. Range ambiguity resolving of HPRF radar based on hybrid filter. Sci China Inf Sci, 2011, 54: 1534–1546, doi: 10.1007/s11432-011-4236-5

1 Introduction

The pulse repetition frequencies (PRF) used by radars vary a lot. When PRF is sufficiently high, range ambiguity will occur, bringing about troubles to radars with high pulse repetition frequency [1]. In order to avoid ambiguity and eliminate the eclipsing loss, multiple PRFs are employed [2, 3].

The present methods for range ambiguity resolving mainly include signal processing methods [4–13] and data processing methods [2, 3, 14–16]. Data processing methods mainly are Chinese Remainder Theorem method, those methods of arranging all the possible ambiguous ranges of mPRFs (used to resolve the range ambiguity) to find the most possible superposition range [2, 3, 16] and multiple hypothesis tracking method [14, 15]. Although Chinese Remainder Theorem method is simple and of low computation complexity, it requires high measuring accuracy and special choice of the PRF [2]. The methods of arranging all the possible ambiguous ranges of mPRFs to find the most possible superposition range is of high computation complexity. Multiple hypothesis tracking method shown in passive target tracking

*Corresponding author (email: hardbonnie@gmail.com)

[17, 18] can realize the target state estimation using probability summation when only one PRF has target measurement in each dwell. However, the simulation results demonstrate that when only one PRF detects the target, multiple hypothesis method converges slowly, and moreover, it will make a mistake sometimes when pulse interval number (PIN) changes.

In this paper, based on the research of [15], PIN and its incremental variable are considered as discrete components of the target state. We try to firstly, find out the correct hypothesis interval by utilizing multiple PRFs based on Euclidean distance, and then to achieve the PIN estimate by hybrid filtering method using one PRF to realize the range ambiguity resolving. Simulation results demonstrate that the proposed method can overcome not only the influence of the measurement error, but also the deficiency of the multiple hypothesis method which converges slowly when only one PRF detects the target and will make a mistake on range ambiguity resolving when PIN changes.

2 Problem formulation

$R_{\max}$ is assumed to be the maximum range of interest, and the set of HPRFs is denoted by F_{ri}, $i = 1, \ldots, I$. Suppose the ith HPRF, F_{ri} among this set, is selected. The corresponding maximum unambiguous range R_{iu} is given by

$$R_{iu} = C/(2 \times F_{ri}), \tag{1}$$

where C is the speed of light.

As illustrated in Figure 1, given the ambiguous range measurement $r_i(k)$ at time k, all possible ranges $r_{il_i}(k)$, $l_i = 1, \ldots, L_i + 1$ are generated by

$$r_{il_i}(k) = (l_i - 1) \times R_{iu} + r_i(k), \quad l_i = 1, \ldots, L_i + 1, \tag{2}$$

where $L_i = \mathrm{Int}(R_{\max}/R_{iu})$ and the function $\mathrm{Int}(\cdot)$ means to take the closest integer of the variable and l_i is PIN to describe range ambiguity.

As shown in Figure 1, range measurement will appear to be only $r_{i1}(k)$. Although there is no direct way of telling which is the true range among $r_{il_i}(k)$, $l_i = 1, \ldots, L_i + 1$, the true range must be one of them, i.e., l_i must be one of $L_i + 1$ numbers [1]. Thus, the key issue of the range ambiguity resolving problem is to estimate the PIN l_i. Since on one hand, with the unknown PIN term, it is difficult to determine the true target position; on the other hand, the estimate of l_i depends on the target's true position. Therefore, it is necessary to provide an integrated approach to the joint estimation of the target state and PIN. Since the base states of the target such as positions and velocities are continuous, while the value of l and its incremental variable are discrete, it is natural to consider the problem of range ambiguity resolving as a hybrid estimation problem.

3 Hybrid state model

In this section, we will formulate a model that allows for the simultaneous estimation of the continuous base states of the target and the discrete range ambiguity state of the system. It is assumed that 2-D radar detector is located at the origin of the coordinate system and a single non-maneuvering target is considered in tracking and range ambiguity resolving. Shown in Figure 2 is a general block diagram of the hybrid system scheme.

3.1 Dynamic stochastic process model

Assume that the state vector of the target at time step k is

$$\boldsymbol{x}_T(k) = \begin{bmatrix} x(k) & \dot{x}(k) & y(k) & \dot{y}(k) \end{bmatrix}', \tag{3}$$

where $(x(k), y(k))$ and $(\dot{x}(k), \dot{y}(k))$ denote the position and velocity of the target respectively.

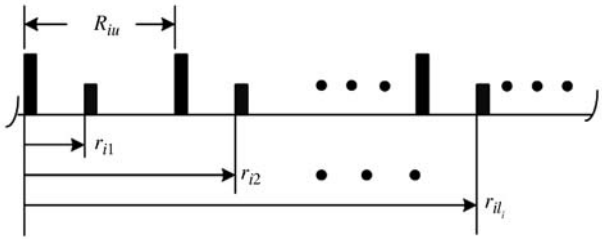

Figure 1 All possible ranges from one range measurement.

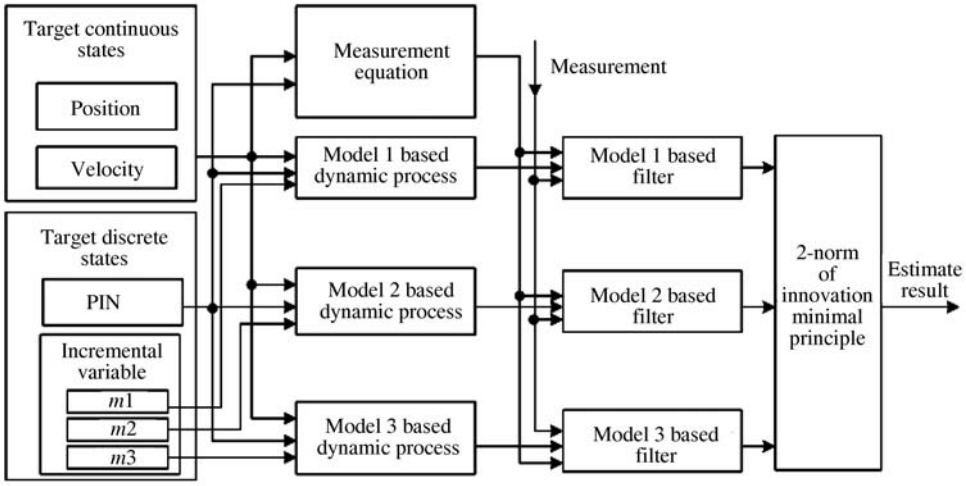

Figure 2 Block diagram of the hybrid system scheme.

The dynamic equation of the non-maneuvering target is

$$\boldsymbol{x}_T(k+1) = \boldsymbol{F}_T(k)\boldsymbol{x}_T(k) + \boldsymbol{G}_T(k)\boldsymbol{V}_T(k), \tag{4}$$

where the transition matrix $\boldsymbol{F}_T(k)$ and $\boldsymbol{G}_T(k)$ are defined respectively as

$$\boldsymbol{F}_T(k) = \begin{bmatrix} 1 & T & 0 & 0 \\ 0 & 1 & 0 & 0 \\ 0 & 0 & 1 & T \\ 0 & 0 & 0 & 1 \end{bmatrix}, \tag{5}$$

and

$$\boldsymbol{G}_T(k) = \begin{bmatrix} T^2/2 & T & 0 & 0 \\ 0 & 0 & T^2/2 & T \end{bmatrix}'. \tag{6}$$

T is the sampling interval, and $\boldsymbol{V}_T(k)$ is a zero-mean white process noise characterized by

$$E\{\boldsymbol{V}_T(k)\boldsymbol{V}_T(j)'\} = \begin{cases} \boldsymbol{Q}_T(k), & k = j, \\ 0, & k \neq j. \end{cases} \tag{7}$$

By considering $l(k)$ and its incremental variable $\Delta l(k)$ as components of the target state, their dynamic equation at time k can be modeled according to

$$\boldsymbol{x}_P(k+1) = \boldsymbol{F}_P(k)\boldsymbol{x}_P(k) + \boldsymbol{V}_P(k), \tag{8}$$

where $\boldsymbol{V}_P(k)$ is a small process noise term with zero-mean and variance $Q_P(k)$, and the ambiguity vector $\boldsymbol{x}_P(k)$ and the transition matrix $\boldsymbol{F}_P(k)$ are obtained respectively as follows:

$$\boldsymbol{x}_P(k) = \begin{bmatrix} l(k) & \Delta l(k) \end{bmatrix}', \tag{9}$$

and

$$\boldsymbol{F}_P(k) = \begin{bmatrix} 1 & 1 \\ 0 & 1 \end{bmatrix}. \tag{10}$$

Let

$$\boldsymbol{x}_{Aug}(k) = \begin{bmatrix} \boldsymbol{x}_T(k) \\ \boldsymbol{x}_P(k) \end{bmatrix}, \quad \boldsymbol{F}_{Aug}(k) = \begin{bmatrix} \boldsymbol{F}_T(k) & 0 \\ 0 & \boldsymbol{F}_P(k) \end{bmatrix}, \quad \boldsymbol{V}_{Aug}(k) = \begin{bmatrix} \boldsymbol{G}_T(k)\boldsymbol{V}_T(k) \\ \boldsymbol{V}_P(k) \end{bmatrix}. \tag{12}$$

The dynamic stochastic process model for this hybrid system can be written as

$$\begin{bmatrix} \boldsymbol{x}_T(k+1) \\ \boldsymbol{x}_P(k+1) \end{bmatrix} = \begin{bmatrix} \boldsymbol{F}_T(k) & 0 \\ 0 & \boldsymbol{F}_P(k) \end{bmatrix} \begin{bmatrix} \boldsymbol{x}_T(k) \\ \boldsymbol{x}_P(k) \end{bmatrix} + \begin{bmatrix} \boldsymbol{G}_T(k)\boldsymbol{V}_T(k) \\ \boldsymbol{V}_P(k) \end{bmatrix}, \tag{12}$$

or equivalently

$$\boldsymbol{x}_{Aug}(k+1) = \boldsymbol{F}_{Aug}(k)\boldsymbol{x}_{Aug}(k) + \boldsymbol{V}_{Aug}(k). \tag{13}$$

Without loss of generality, it is assumed that the target cannot jump out of one maximum unambiguous range in one time interval. Thus the state model of $l(k)$ can be reasonably simplified into

$$l(k+1) = \begin{cases} l(k)+1, & \text{when target goes forward to the next } R_u, \\ l(k), & \text{when target remains in this } R_u, \\ l(k)-1, & \text{when target goes backward to the previous } R_u, \end{cases} \tag{14}$$

where R_u is the maximum unambiguous range for the current HPRF.

Therefore, we have

$$\Delta l(k) = l(k+1) - l(k) = \begin{cases} 1, & \text{when target goes forward to the next } R_u, \\ 0, & \text{when target remains in this } R_u, \\ -1, & \text{when target goes backward to the previous } R_u. \end{cases} \tag{15}$$

By eq. (15), $\Delta l(k)$ can take one discrete value out of the set of candidates $\{-1, 0, 1\}$ at a random time step.

There are two methods to deal with the hybrid state estimation as follows. The first method is to estimate $\Delta l(k)$ directly by EKF using eq. (13). However, the thresholds are required to get the discrete value of $\Delta l(k)$ because its estimate by EKF is continuous. Therefore, this method needs to choose the threshold.

The second method is to diminish the target hybrid state vector as five-dimensional state vector based on the fact that $\Delta l(k)$ is taken from a set of known candidates. The target hybrid state vector can be diminished into

$$\boldsymbol{x}(k) = \begin{bmatrix} x(k) & \dot{x}(k) & y(k) & \dot{y}(k) & l(k) \end{bmatrix}', \tag{16}$$

and eq. (13) is equivalent to

$$\boldsymbol{x}(k+1) = \boldsymbol{F}(k)\boldsymbol{x}(k) + \boldsymbol{B}\Delta l(k) + \boldsymbol{V}(k), \tag{17}$$

where

$$\boldsymbol{F}(k) = \begin{bmatrix} 1 & T & 0 & 0 & 0 \\ 0 & 1 & 0 & 0 & 0 \\ 0 & 0 & 1 & T & 0 \\ 0 & 0 & 0 & 1 & 0 \\ 0 & 0 & 0 & 0 & 1 \end{bmatrix}, \quad \boldsymbol{V}(k) = \begin{bmatrix} \boldsymbol{G}_T(k)\boldsymbol{V}_T(k) \\ u(k) \end{bmatrix}, \quad \boldsymbol{B} = \begin{bmatrix} 0 \\ 0 \\ 0 \\ 0 \\ 1 \end{bmatrix}. \tag{18}$$

$u(k)$ is a small process noise with zero-mean and variance $Q(k)$ as will be deduced in Appendix 1.

Since $\Delta l(k)$ takes three discrete values, eq. (17) may have three different models accordingly:

$$\begin{cases} M1: & \boldsymbol{x}(k+1) = \boldsymbol{F}(k)\boldsymbol{x}(k) + \boldsymbol{B} + \boldsymbol{V}(k), & \text{when } \Delta l(k) = 1, \\ M2: & \boldsymbol{x}(k+1) = \boldsymbol{F}(k)\boldsymbol{x}(k) + \boldsymbol{V}(k), & \text{when } \Delta l(k) = 0, \\ M3: & \boldsymbol{x}(k+1) = \boldsymbol{F}(k)\boldsymbol{x}(k) - \boldsymbol{B} + \boldsymbol{V}(k), & \text{when } \Delta l(k) = -1. \end{cases} \tag{19}$$

In order to avoid the choice of the threshold, the second method is adopted to estimate the hybrid state.

3.2 Measurement model

The measurement equation of the target for the ith HPRF at time k takes the form

$$\boldsymbol{z}_i(k) = h(\boldsymbol{x}(k)) + \boldsymbol{W}(k), \tag{20}$$

where $\boldsymbol{W}(k)$ is zero-mean, white Gaussian noise with known covariance $\boldsymbol{R}(k)$ defined as

$$\boldsymbol{R}(k) = \begin{bmatrix} \sigma_r^2 & 0 \\ 0 & \sigma_\theta^2 \end{bmatrix}, \tag{21}$$

with range and azimuth measurement errors σ_r and σ_θ,

$$\boldsymbol{z}_i(k) = \begin{bmatrix} r_i(k) \\ \theta_i(k) \end{bmatrix}, \tag{22}$$

and

$$h(\boldsymbol{x}(k)) = \begin{bmatrix} \sqrt{x(k)^2 + y(k)^2} - (l_i(k) - 1) \times R_{iu} \\ \arctan\left(\frac{x(k)}{y(k)}\right) \end{bmatrix}. \tag{23}$$

Therefore, the hybrid system can be described as three filtering systems by eqs. (19) and (20).

4 Range ambiguity resolving algorithm based on hybrid estimation

Range ambiguity resolving problem can be formulated as a hybrid estimation scheme, in which three filters run in parallel. In this section, based on the hybrid state model obtained in section 3, the range ambiguity resolving algorithm is given.

4.1 Algorithm process

Assume that the tracking time step is K, and the algorithm process is as follows.

1. Hybrid state initialization. In the initial two time steps, the initial state estimate $\hat{\boldsymbol{x}}_m(0|0), m = 1, 2, 3$ takes the same value which will be given in subsection 4.2 and $P_m(0|0), m = 1, 2, 3$ also takes the same value given by eq. (24) deduced in Appendix 2.

$$P_m(0|0) = \begin{bmatrix} r^{11} & r^{11}/T & r^{12} & r^{12}/T & 0 \\ r^{11}/T & 2r^{11}/T^2 & r^{12}/T & 2r^{12}/T^2 & 0 \\ r^{12} & r^{12}/T & r^{22} & r^{22}/T & 0 \\ r^{12}/T & 2r^{12}/T^2 & r^{22}/T & 2r^{22}/T^2 & 0 \\ 0 & 0 & 0 & 0 & Q(k) \end{bmatrix}, \quad m = 1, 2, 3. \tag{24}$$

The following algorithm starts from $k = 1$.

2. State transformation between different HPRFs. If the measurement at time step k comes from the same HPRF as that of the measurement at time step $k-1$, jump to step 3 directly; otherwise, obtain the target state estimation of the HPRF at time step $k-1$ which gets the estimation at time step k by the method given in subsection 4.3.

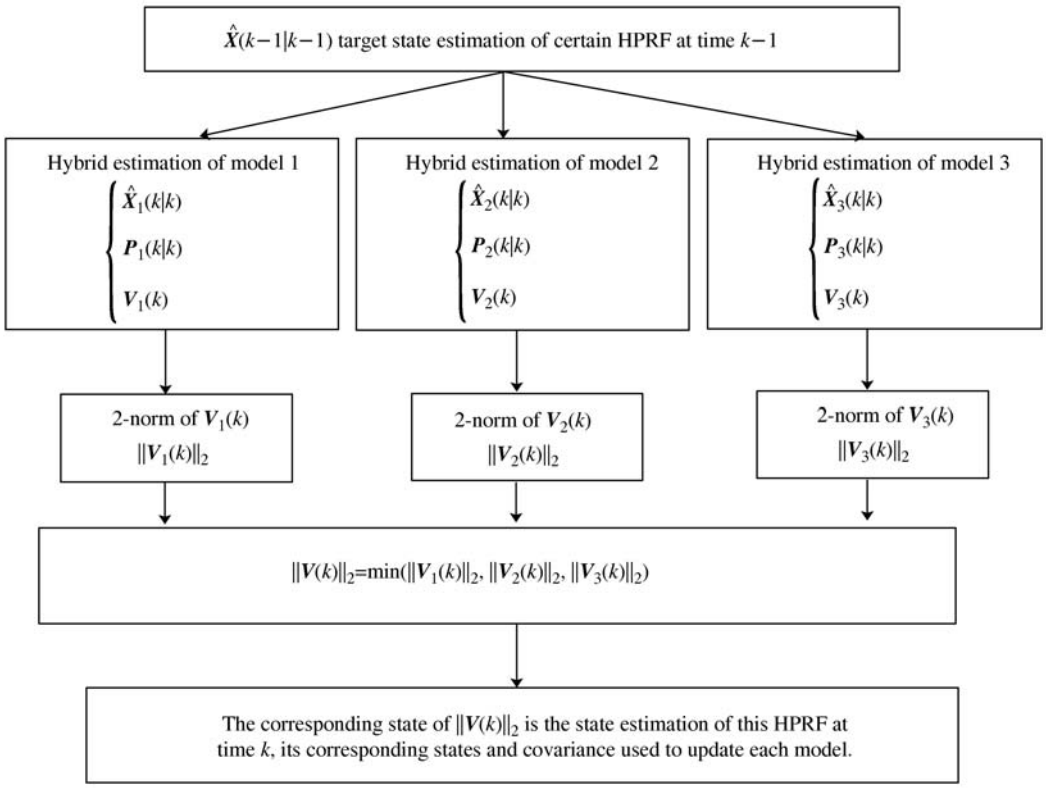

Figure 3 One cycle of the hybrid estimate process.

3. One cycle of the hybrid estimation. As shown in Figure 3 the estimation goes as follows: Firstly, obtain the state and covariance estimation for each model based on the measurements at time step k; then get 2-norm of the innovation for each model as

$$\|\boldsymbol{V}(k)\|_2 = (|\boldsymbol{V}^{11}(k)|^2 + |\boldsymbol{V}^{21}(k)|^2)^{\frac{1}{2}}, \tag{25}$$

next get the minimal 2-norm by comparison; finally, update each model using the target estimation of the model with the minimal 2-norm.

4. If $k = K$, end; if $k < K$, $k = k + 1$, return to step 2.

4.2 Hybrid state initialization

At time k, for the ith HPRF F_{ri}, $i = 1, \ldots, I$ all possible ranges can be obtained from eq. (2), thus all of the possible measurements can be given by

$$\boldsymbol{z}_{il_i}(k) = (r_{il_i}(k), \theta_i(k)), \quad i = 1, \ldots, I, \quad l_i = 1, \ldots, L_i + 1. \tag{26}$$

The l_ith possible measurement for the ith HPRF in polar coordinate can be transformed into Cartesian coordinate by

$$\boldsymbol{z}^C_{il_i}(k) = \begin{bmatrix} z^{C11}_{il_i}(k) \\ z^{C21}_{il_i}(k) \end{bmatrix} = \begin{bmatrix} r_{il_i}(k) \times \cos(\theta_i(k)) \\ r_{il_i}(k) \times \sin(\theta_i(k)) \end{bmatrix}, \quad i = 1, \ldots, I,\ l_i = 1, \ldots, L_i + 1. \tag{27}$$

Then, the initial hybrid state estimate is

$$\hat{\boldsymbol{x}}_{il_i}(0) = \left[z^{C11}_{il_i}(0), \frac{z^{C11}_{il_i}(0) - z^{C11}_{il_i}(-1)}{T}, z^{C21}_{il_i}(0), \frac{z^{C21}_{il_i}(0) - z^{C21}_{il_i}(-1)}{T}, l_i \right]',$$
$$\forall\ l_i = 1, \ldots, L_i + 1;\ i = 1, \ldots, I, \tag{28}$$

where $z_{il_i}^C(-1)$ and $z_{il_i}^C(0)$ are the measurements in the initial two time steps respectively.

Due to ambiguous range measurement, multiple HPRFs are used to get the initial hybrid state estimate based on the fact that the correct range measurements obtained from multiple HPRFs should be the same without considering measurement error. However, considering the measurement error, the Euclidean distance of the initial state estimates from multiple HPRFs should be compared to get the initial state estimate for the hybrid estimate. The Euclidean distance between two possible initial state estimates is calculated as follows:

$$d(\hat{\boldsymbol{x}}_{il_i}(0), \hat{\boldsymbol{x}}_{jl_j}(0)) = \|\hat{\boldsymbol{x}}_{il_i}(0) - \hat{\boldsymbol{x}}_{jl_j}(0)\| = [(\hat{\boldsymbol{x}}_{il_i}^{11}(0) - \hat{\boldsymbol{x}}_{jl_j}^{11}(0))^2 + (\hat{\boldsymbol{x}}_{il_i}^{31}(0) - \hat{\boldsymbol{x}}_{jl_j}^{31}(0))^2]^{\frac{1}{2}},$$
$$\forall i, j \in 1, \ldots, I;\ l_i = 1, \ldots, L_i + 1;\ l_j = 1, \ldots, L_j + 1. \tag{29}$$

Then, the initial state estimate can be obtained from the minimum distance as follows:

$$(m, p, n, q) = \arg \min_{\substack{\forall i,j \in 1,\ldots,I \\ l_i = 1,\ldots,L_i+1 \\ l_j = 1,\ldots,L_j+1}} \{d(\hat{\boldsymbol{x}}_{il_i}(0), \hat{\boldsymbol{x}}_{jl_j}(0))\}. \tag{30}$$

Thus, the initial state estimates of the mth and nth HPRF are

$$\hat{\boldsymbol{x}}_m(0) = \hat{\boldsymbol{x}}_{mp}(0), \quad \hat{\boldsymbol{x}}_n(0) = \hat{\boldsymbol{x}}_{nq}(0), \tag{31}$$

and the hybrid state initialization is obtained by

$$\hat{\boldsymbol{x}}(0) = \hat{\boldsymbol{x}}_m(0) \ \text{ or } \ \hat{\boldsymbol{x}}(0) = \hat{\boldsymbol{x}}_n(0). \tag{32}$$

When only one HPRF detects the target, by eq. (28), the initial state estimation of each hypothesis interval can be achieved by the measurements obtained by one HPRF in the initial two time steps.

4.3 State transformation between different HPRFs

Airborne radars employ multiple HPRFs to resolve range ambiguity. When switching HPRF, it can only influence the value of $l(k)$. Thus, $l(k)$ should be reevaluated.

It is assumed that in the tracking maintenance, if the ith HPRF at time step $k-1$ switches to the jth HPRF at time step k, the state of the HPRF at time step $k-1$ should be reevaluated. The PIN of the jth HPRF can be obtained by

$$l_j(k-1) = \text{Int}(\sqrt{(\hat{\boldsymbol{x}}^{11}(k-1))^2 + (\hat{\boldsymbol{x}}^{31}(k-1))^2}/R_{ju}), \tag{33}$$

where $\hat{\boldsymbol{x}}(k-1)$ is the state estimate at the time step $k-1$ and R_{ju} is the maximum unambiguous range for the jth HPRF. Thus, the hybrid state estimation of the jth HPRF at time step $k-1$ is

$$\hat{\boldsymbol{x}}_j(k-1) = [\hat{\boldsymbol{x}}^{11}(k-1), \hat{\boldsymbol{x}}^{21}(k-1), \hat{\boldsymbol{x}}^{31}(k-1), \hat{\boldsymbol{x}}^{41}(k-1), l_j(k-1)]'. \tag{34}$$

In actual tracking process, the target state transformation can be obtained by eqs. (33) and (34) between different HPRFs.

5 Simulation results and analysis

In this section, 2-D tracking examples where a single target is moving with constant velocity are presented to demonstrate the algorithm proposed for range ambiguity resolving. The maximum range $R_{\max}$ is 200 km. The sampling interval $T = 1$ s and tracking step $K = 25$. The measurement errors σ_r=100 m and $\sigma_\theta = 0.5°$. The process noise covariance $Q_T(k) = (10\ \text{m})^2$. For convenience, pulse repetition interval (PRI) is used here to substitute PRF. Monte Carlo takes 100.

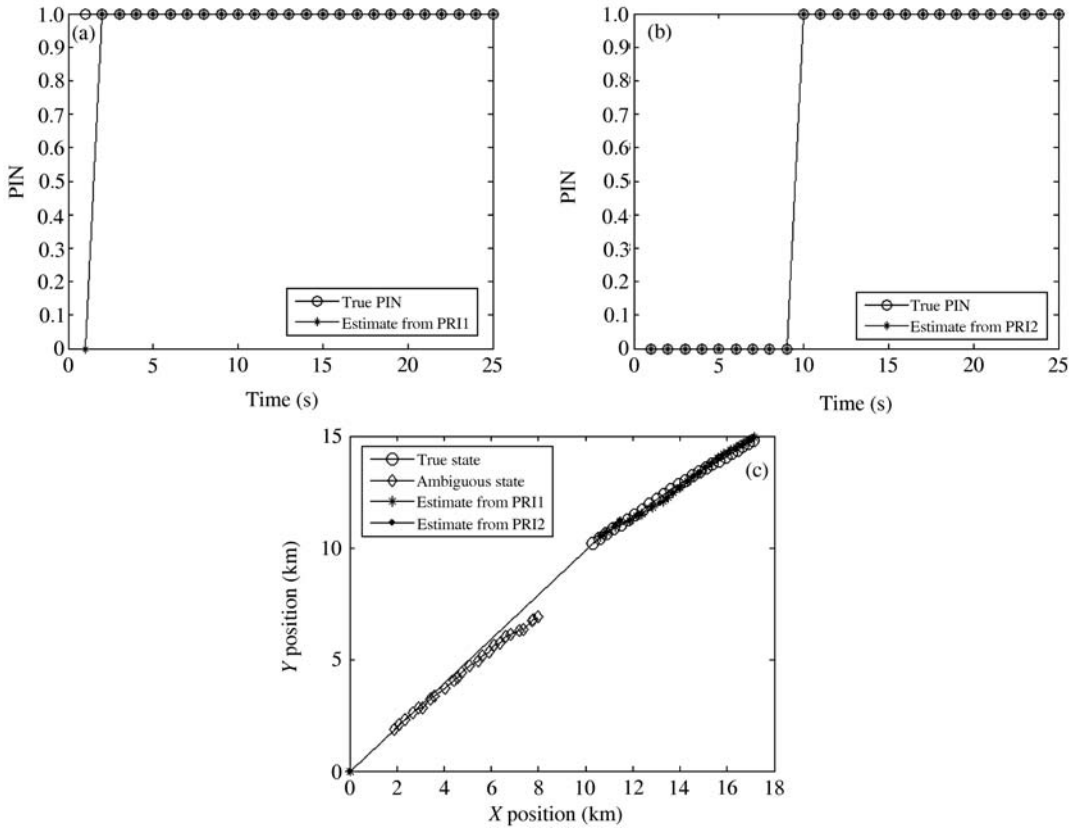

Figure 4 Simulation results. (a) PIN estimate from PRI1; (b) PIN estimate from PRI2; (c) target position estimation.

The velocity of the target is assumed to be (0.3 km/s, 0.2 km/s) and the initial position is (10 km, 10 km). PRI1=80 μs and PRI2=120 μs. The simulation results are given in Figure 4. Figures 4(a) and 4(b) present the estimation of PIN respectively and Figure 4(c) displays the tracking result. Moreover, the root-mean-squared errors (RMSEs) of target position are partly given in Table 1. Figure 4(a) shows that when the initial position of the target is ambiguous for PRI1, the estimates of PIN are correct in the tracking process except for the first time step. Figure 4(b) shows that when the initial position of the target is unambiguous for PRI2, the estimates of PIN are always correct in the tracking process. The reason is that $l(k)$ is predefined as zero in the simulation. Figure 4(c) displays that based on the correct estimate of PIN, the algorithm can track the target successfully. It can be seen from Table 1 that for both of the PRIs, from the time step 2, the RMSEs of the target position are within 700 m and converges within 200 m, while the maximum unambiguous ranges of PRI1 and PRI2 are 12 and 8 km respectively; therefore tracking accuracy is high.

The simulation results demonstrate that

1. Whether the initial position of the target is ambiguous for the current PRF or not, the algorithm can deal with the range ambiguity resolving successfully.

2. The position accuracy of the algorithm is high.

In the following subsections, the theoretical development will be verified further by simulations with different parameters such as velocity of the target, PRI and measurement error. Moreover, the simulation comparison between the proposed method and the multiple hypothesis method is given.

5.1 Position RMSE on the conditions of different velocities of the target

Assume that the velocity of the target varies from (0.2 km/s, 0.2 km/s) to (1.2 km/s, 1.2 km/s). Table 2 shows the position RMSEs with different velocities partly.

From Table 2, we reach the following conclusions:

1. The higher the velocity is, the larger the RMSE will be.

Table 1 The position RMSEs (km)

PRI (μs)	Time (s)								
	2	3	4	5	6	7	8	9	10
PRI1	0.15044	0.28184	0.3262	0.30856	0.26391	0.24302	0.219	0.19263	0.17298
PRI2	0.15044	0.45396	0.61377	0.44895	0.37758	0.32272	0.26659	0.21521	0.17485

Table 2 The position RMSEs with different velocities (km)

Time (s)	Velocity (km/s)					
	0.2	0.4	0.6	0.8	1	1.2
21	0.10014	0.11867	0.12636	0.18378	0.15154	0.21161
22	0.10080	0.11504	0.12994	0.17134	0.15549	0.20373
23	0.10294	0.11419	0.13064	0.15347	0.16063	0.18344
24	0.10193	0.11603	0.13363	0.14858	0.17947	0.17356
25	0.10173	0.11789	0.1364	0.14974	0.20047	0.17657

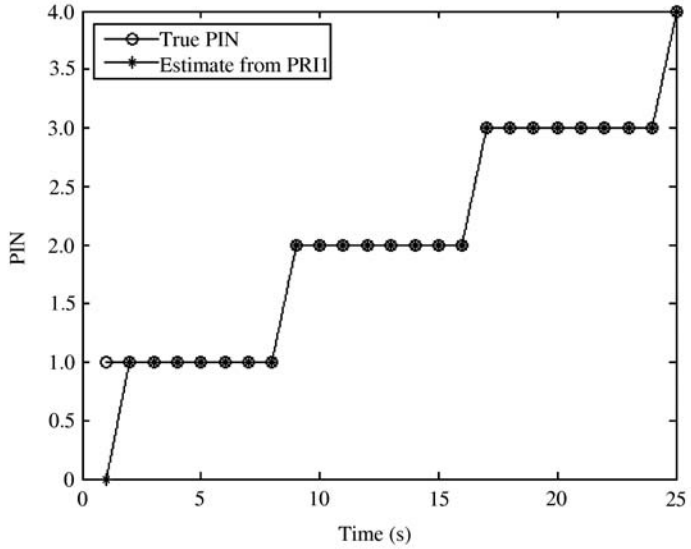

Figure 5 PIN estimate with [1 km/s, 1 km/s].

2. When PIN of PRI changes, the RMSE of the position will increase. For example, when the velocity of the target is (1 km/s, 1 km/s), RMSE is 0.2007 at time step 25, which is larger than that with the velocity of (1.2 km/s, 1.2 km/s). As shown in Figure 5, PIN changes at the time step 25 for PRI1 when target takes (1 km/s, 1 km/s).

5.2 Position RMSE on the conditions of different PRIs

Table 3 shows the position RMSEs of different PRIs partly. The smaller PRI is, i.e., the higher PRF is, the larger the RMSE will be.

5.3 Position RMSE on the conditions of different measurement errors

When the range measurement error varies from 100 to 300 m and the azimuth measurement error takes 1° and 2°, Table 4 shows the position RMSEs partly.

From Table 4, we conclude

1. With larger RMSE, the proposed algorithm can still deal with range ambiguity resolving. For example, when measurement errors are (300 m, 2°), RMSE can converge within 0.4 km, while the maximum unambiguous range is 12 km, and the algorithm can realize the ambiguity resolving.

Table 3 The position RMSEs of different PRIs (km)

PRI (μs)	PRI1	80	40	37	27
	PRI2	100	60	50	50
Time (s)	20	0.098169	0.12181	0.21377	0.39788
	21	0.10049	0.12178	0.21927	0.41235
	22	0.099452	0.11964	0.21206	0.42738
	23	0.10095	0.12088	0.21752	0.42363
	24	0.10233	0.12358	0.22846	0.41575
	25	0.10267	0.12415	0.22495	0.41039

Table 4 The position RMSEs with different measurement errors (km)

Error	Range (m)	100	100	200	200	300	300
	Azimuth(°)	1	2	1	2	1	2
Time (s)	21	0.1447	0.23197	0.16534	0.26058	0.33298	0.41257
	22	0.15412	0.23417	0.16934	0.25981	0.33973	0.41567
	23	0.15201	0.23716	0.16847	0.26082	0.35031	0.39527
	24	0.14766	0.22503	0.16476	0.25265	0.33807	0.38823
	25	0.14733	0.23395	0.16365	0.25245	0.34164	0.38713

2. The larger the range measurement error is, the larger the RMSE will be. For example, at the time step 25, when measurement errors are (100 m, 1°), RMSE is 0.14733 km; when measurement errors are (300 m, 1°), RMSE is 0.34164 km.

3. The larger the azimuth measurement error is, the larger the RMSE will be. For example, at the time step 25, when measurement errors are (100 m, 1°), RMSE is 0.14733 km; when measurement errors are (100 m, 2°), RMSE is 0.23395 km.

5.4 Comparison with the multiple hypothesis method

In this subsection, it is assumed that PRI1 and PRI2 take 153 and 172 μs respectively and 153 μs is chosen for hybrid filtering algorithm, $K = 30$. Since initialization is realized in the initial two time steps, the simulation results are given from the third time step. When only one HPRF detects the target at each time step, the tracking results and the position RMSE obtained by two methods are given in Figure 6(a) and (b) respectively. When two HPRFs detect the target, the tracking results and the position RMSE are given in Figure 6(c) and (d) respectively. The PIN estimate of PRI1 obtained by the proposed method for both cases is shown in Figure 6(e).

As is evident in Figure 6(a) and (b), when only one HPRF detects the target, the multiple hypothesis method requires several time steps to converge to the correct state, while the proposed method can track the target since the third time step. When PIN changes at the time step 10 (see Figure 6(e)), the position RMSE obtained by the multiple hypothesis method increases abruptly at the time step 10, and it will make a mistake on target tracking, while the position RMSE of the proposed method is small and stable, thus being able to deal with the range ambiguity resolving without considering the influence of PIN variation (see Figure 6(b) and (c)).

6 Conclusions

The main contribution of this paper is converting range ambiguity resolving problem into a hybrid state estimation problem, with the discrete-valued PIN and its incremental variable considered as target states. The effectiveness of the proposed method in the range ambiguity resolving is verified by simulations of different HPRFs with different parameters. Simulation results show that the target position RMSE of the method will be smaller with lower HPRF, lower velocity or higher measurement accuracy. Moreover, the method proposed in this paper can converge more rapidly than multiple hypothesis method when only one HPRF detects the target without making any mistake when PIN changes.

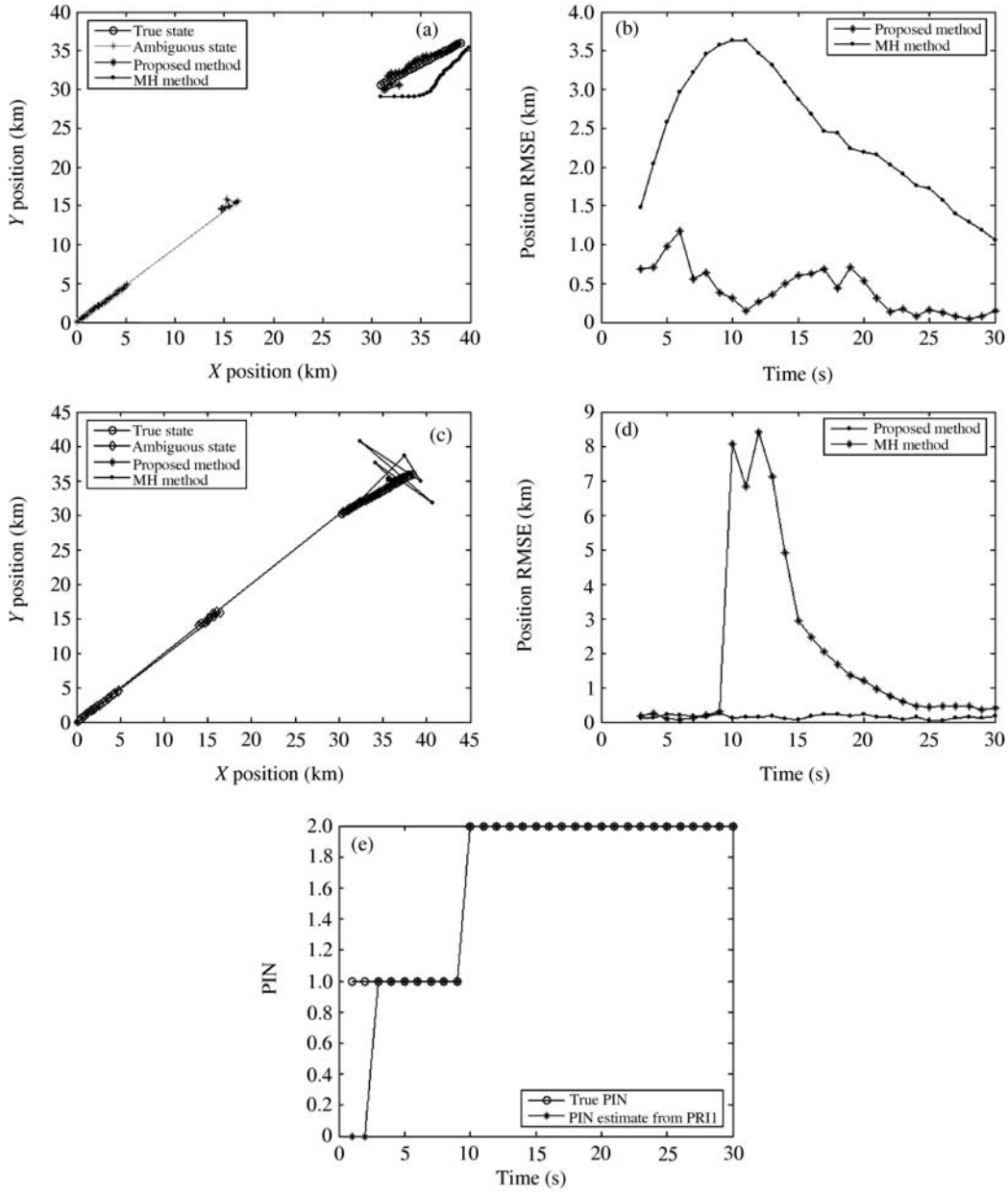

Figure 6 Simulation results. (a) When only one PRF detects target, tracking results of the two methods; (b) when only one PRF detects target, position RMSE of the two methods; (c) when two PRFs detect target, tracking results of the two methods; (d) when two PRFs detect target, position RMSE of the two methods; (e) PIN estimate of PRF1 on two cases.

Acknowledgements

This work was supported by the Foundation for the Author of National Excellent Doctoral Dissertation of China (Grant No. 200443), the National Natural Science Foundation of China (Grant Nos. 60972159, 61032001, 61002006), and Special Foundation Program for Mountain Tai Scholars.

References

1 Stimson G W. Introduction to Airborne Radar. New Jersey: SciTech Publishing, 1998. 153–154

2 Wang J M, Yang J, Wu S J. A new algorithm of range ambiguity resolution for Pulse Doppler radar (in Chinese). Radar & ECM, 2005, 3: 38–41

3 Jiang K, Li M. A novel algorithm for PD radar range resolving ambiguity (in Chinese). Fire Control Radar Technol, 2008, 37: 25–28
4 Li L, Ren L X, He P K, et al. Study on range window in HPRF stepped frequency radar system. In: Proceedings of the 9th International Conference on Signal Processing, Beijing, China, 2008. 2501–2504
5 Ren L X, Mao E K. Study on HPRF Pulsed Doppler stepped frequency radar system. In: Proceedings of the 6th CIE International Conference on Radar, Shanghai, China, 2006. 1–4
6 Strecker A, Wieszt A, Al-youssof N, et al. Method for detecting targets and determining their distance via an HPRF radar system. US Patent, 7 151 481 B1, 2006-12-19
7 Duan J Q, He Z S, Qin L. A new approach for simultaneous range measurement and Doppler estimation. IEEE Geosci Remote Sens Lett, 2008, 5: 492–496
8 Nagel D, Hommel H. A new HPRF mode with highly accurate ranging capability for future airborne radars. In: Proceedings of 2001 CIE International Conference on Radar, Beijing, China, 2001. 275–280
9 Deng H, Himed B, Wicks M C. Concurrent extraction of target range and Doppler information by using orthogonal coding waveforms. IEEE Trans Signal Process, 2007, 55: 3294–3301
10 Lin F L, Steiner M. New techniques for radar coherent range ambiguity resolution. In: Proceedings of the 2001 IEEE Radar Conference, Atlanta, USA, 2001. 99–104
11 Anderson J, Temple M, Brown W, et al. A nonlinear suppression technique for range ambiguity resolution in Pulse Doppler radars. In: Proceedings of the 2001 IEEE Radar Conference, Atlanta, USA, 2001. 141–146
12 Nadav L. Mitigating range ambiguity in high PRF radar using inter-pulse binary coding. IEEE Trans Aerospace Electron Syst, 2009, 45: 687–697
13 Akhtar J. Cancellation of range ambiguities with block coding techniques. In: Proceedings of 2009 IEEE Radar Conference, Pasadena, USA, 2009. 1–6
14 Liu Z L, Zhang G Y, Xu Z L, et al. Multiple hypothesis track algorithm for airborne fire control radar with HPRF in FMR mode (in Chinese). Acta Armamentarii, 2007, 28: 431–435
15 Liu Z L, Guo Y C, Zhang G Y, et al. Multiple models track algorithm for radar with high pulse-repetition frequency in frequency-modulated ranging mode. IET Radar Sonar Nav, 2007, 1: 1–7
16 Zhang G, Zhu Z D, Lu B. Parallel realization of multi-slide window algorithm on DSP (in Chinese). J Data Acquisition Process, 2002, 17: 209–212
17 Kronhamn T R. Bearings-only target motion analysis based on a multi-hypothesis Kalman filter and adaptive ownship motion control. IEE Proc Radar Sonar Navig, 1998, 145: 247–252
18 Peach N. Bearings-only tracking using a set of range-parameterized extended Kalman filters. IEEE Proc Control Theory Appl, 1995, 142: 73–80
19 Li X R, Jilkov V P. Overview of multiple-model methods for maneuvering target tracking. SPIE, 2003, 5204: 200–210
20 He Y, Xiu J J, Zhang J W, et al. Radar Data Processing with Applications (in Chinese). Beijing: Publishing House of Electronics Industry, 2006

Appendix 1 Calculating the variance of the PIN $l_i(k)$ for the ith HPRF

$l_i(k)$ is a discrete random variable, which can take a random value at any time instant from the set of $\{1, 2, \ldots, L_i+1\}$ with equal probability $\frac{1}{L_i+1}$.

First, the expected value can be obtained as follows:

$$\mu_{l_i} = E(l_i) = \frac{1}{L_i+1}\sum_{j=1}^{L_i+1} l_{ij}. \tag{A1}$$

Then, the variance $Q(k)$ of $l_i(k)$ is given by

$$Q(k) = E[(l_{ij}-\mu_{l_i})^2] = \frac{1}{L_i+1}\sum_{j=1}^{L_i+1}(l_{ij}-\mu_{l_i})^2. \tag{A2}$$

Appendix 2 Covariance of the initial state estimate [20]

Since measurement noise variance in Polar Coordinate is

$$\boldsymbol{R} = \begin{bmatrix} \sigma_r^2 & 0 \\ 0 & \sigma_\theta^2 \end{bmatrix}, \tag{A3}$$

and its measurement noise variance in Cartesian coordinate reads

$$\boldsymbol{R}^C(0|0) = \begin{bmatrix} r^{11} & r^{12} \\ r^{21} & r^{22} \end{bmatrix} = \boldsymbol{ARA}, \tag{A4}$$

where

$$\boldsymbol{A} = \begin{bmatrix} \cos\theta(0) & -r(0)\sin\theta(0) \\ \sin\theta(0) & r(0)\cos\theta(0) \end{bmatrix}, \tag{A5}$$

thus the initial covariance matrix can be obtained by eqs. (A2) and (A4)

$$P(0|0) = \begin{bmatrix} r^{11} & r^{11}/T & r^{12} & r^{12}/T & 0 \\ r^{11}/T & 2r^{11}/T^2 & r^{12}/T & 2r^{12}/T^2 & 0 \\ r^{12} & r^{12}/T & r^{22} & r^{22}/T & 0 \\ r^{12}/T & 2r^{12}/T^2 & r^{22}/T & 2r^{22}/T^2 & 0 \\ 0 & 0 & 0 & 0 & Q(k) \end{bmatrix}. \tag{A6}$$